Description of main S & T results / foregrounds

Summary

The research activities within SIKELOR were focused on three different key aspects, whereby the following main results have been achieved:

I) Development of a technology for cleaning and densification of the kerf loss and the production of compacted bodies for further processing

- A pilot plant has been established at GARBO for cleaning and compaction of the silicon kerf loss.
- The pilot plant achieves a capacity of 7 kg/day of recycled silicon.
- A quality control system for the compacted silicon bodies has been installed.
- Total unitary costs for a 2000 MT/year silicon plant add up to 4.39 EUR/kg for the recycled silicon. These costs are well below the target price thus making the business of the kerf loss recovery highly attractive.
- The recycled silicon feedstock was delivered to UNIPD as starting material for the crystallization experiments.

II) Numerical and experimental modelling for identifying optimal process parameters for electromagnetic processing

- Calculations of flow and temperature fields, particle distributions and separation probabilities were performed by UNIG for both demonstrators
- Contrary to initial expectations an efficient separation of SiC particles in G1 or G2.5 geometry requires higher frequencies as reported in the literature.
- Flow fields at high shielding parameters differ significantly from well-known time-averaged flow structures referred in the literature. Complex, transient vortex structures occur and prove a significant mixing effect by the alternating magnetic field.
- A recipe for the crystallization experiments has been proposed in terms of an optimized set of magnetic field parameters and procedures. The simulations demonstrate a significant separation effect in the G1 experiment in Demonstrator II.

III) Implementation of the Demonstrator on laboratory scale and accomplishment of crystallization experiments

- Two different experiments offering the G2.5 and the G1 geometry, respectively, were realized in the Demonstrator II considering. Powerful and efficient magnetic field systems for both experiments were designed by UNIPD.
- A completely new design for hot zone and inductor was made for the G1 experiment.
- A new power supply was designed and implemented by EAAT for Demonstrator II.
- Crystallization experiments were performed successfully in the Demonstrator II using the recycled feedstock from GARBO

A brief description of the work conducted within SIKELOR in line with these key aspects will be presented below. For a more detailed description we refer to the Second Periodic Report.

Changes in the research program with respect to the original DoW

New insights made within SIKELOR entailed some significant modifications in the work program with respect to the realization of the Demonstrators I and II.
The Demonstrator II was realized within the *i*DSS furnace in the laboratory of UNIPD. The original plan assumed that three different magnetic field frequencies have to be used for achieving of optimized combinations of induction heating, electromagnetic stirring and

electromagnetic separation. The heating of the silicon requires frequencies in the order of a few kHz whereas the electromagnetic stirring is usually conducted at much lower frequencies not larger than 50 Hz. The information being available from the literature at the starting point of the project indicated an optimal field frequency for an efficient separation to lying in between the frequency ranges for heating and stirring. First investigations and numerical simulations revealed that significantly higher frequencies are necessary for particle separation in large crucibles being in the range of the heating frequencies or even higher. The optimum separation frequency for the particular setup of the *i*DSS furnace is supposed to be approximately 4…6 kHz which is nearly twice the maximum applicable heating frequency of 3 kHz. A straightforward increase of the magnetic field frequency in the molten Si is obstructed by the graphite susceptor due to the shielding effect. A removal of the susceptor or a reduction of the thickness of the graphite plates cannot be allowed because of safety concerns regarding a potential failure of the crucible analysed and formulated in the Deliverable 8.1 "Report on the safety of Demonstrator II". The problem was fixed by the following solution. Two experiments were realized inside the *i*DSS furnace:

1) Large geometry (G2.5)

   The size of the crucible corresponds to the original plan. The investigations consider the influence of inductive heating (until a frequency of 3 kHz) and tailored electromagnetic stirring on the particle migration and separation. Recent studies from the literature and numerical simulations within WP 6 gave cause to the assumption that the engulfment of particles by a propagating solidification front may contribute to particle separation in the edge regions of the sample.

2) Smaller geometry (G1)

   The utilization of a smaller crucible allows for installing a new side inductor for separation in the hot zone. This modification enables to apply higher frequencies up to 6 kHz where the Leenov-Kolin force (LKF) becomes large enough to promote particle separation. This experiment allows for studying the superposition of Leenov-Kolin-force with tailored electromagnetic stirring.

During the work in the second project period further problems became manifest which could only hardly be anticipated at the beginning of SIKELOR. First considerations done in WP 7 revealed that the parameters of the magnetic system in Demonstrator I at GARBO would not allow for a direct separation produced by the LKF. The more realistic scenario for this specific configuration concerns a separation mechanism relying on the particle engulfment of the progressing solidification front. The application of a traveling magnetic field (TMF) is required to realize this approach which feasibility was strongly supported by the results of numerical simulations done by UNIG. A sufficiently strong magnetic field strength has to be generated for achieving minimum fluid velocities. Calculations showed that only an internal metallic coil can be used for that purpose. However, the installation of metal parts in the hot zone involves the risk of contamination. As it is well known that metals are detrimental life-time killers for the minority charge carriers, the idea of producing a metallic coil was abandoned by GARBO. Further efforts were made to consider an optimization of graphite coils towards highest possible field strengths. The results obtained were not convincing. The attainable velocities could reach at best the order of magnitude where the threshold for separation is expected by the numerical simulations. Furthermore, this intensity of fluid flow is not more intense as published in the literature for other large scale crystal growth systems. The scientific outcome of installing the coil system in GARBO's furnace would have been limited since a strong engulfing effect cannot be expected. Analyzing this situation the project partners came to the conclusion to abandon Demonstrator I in the form as initially planned, but, to transfer the project objectives of Demonstrator I to the experiments to be carried out in Demonstrator II. The redundant resources have been redirected to other research activities that

aimed to achieve the project goals by other approaches. The work was reorganized by substituting the work program of Demonstrator I by other tasks, in particular:

- Sintering experiments (GARBO)

The additional sintering procedure improves the density of the compacts allowing a higher crucible filling factor and reduces a certain amount of oxygen yet ahead the electromagnetic processing and casting.

- Feasibility study for performing the experiments planned for Demonstrator I in Demonstrator II (HZDR)

Demonstrator II provides a combination of a TMF and an AMF and thus generally is capable of conducting all experiments foreseen for Demonstrator I with its hardware. The feasibility study showed that in a variety of details, e.g., field strengths, achievable fluid velocity, and problems with the pole pitch, the TMF in Demonstrator II is even superior to the one it was considered in Demonstrator I. All results to be achieved in Demonstrator I regarding fluid flow in a TMF can be also and partly even better done with the hardware of Demonstrator II.

- Support for Demonstrator II (GARBO, HZDR)

A completely new how zone for the *i*DSS furnace is required since the formerly used graphite parts shield most of the magnetic field at the higher frequencies needed. In conjunction with the fact that alone the new hot zone and the new inductor for the G1 experiment exceed by far the budget allocated for Demonstrator II, a re-distribution of the project resources was necessary. A part of the budget of the HZDR and GARBO that released from Demonstrator I was spend on Demonstrator II. Manpower costs from the HZDR planned for Demonstrator I were used to a significant extend for contributions for designing and building the new hot zone for Demonstrator II.

Detailed description of the work

I) Densification of the kerf loss

Compaction of silicon powders is a mandatory step for the recycling of silicon kerf loss from fixed abrasive sawing (FAS) because of the extremely small size of the particles down to the range of 250 nanometers. The utilization of submicron sized powder in casting processes is hindered by technical and safety issues, namely:

- Difficulties in handling the powders and in avoiding cross contamination from materials and environment in contact with the fine silicon;
- Ultra-fine silicon powder are flammable and may form explosive mixtures with air,
- The bulk density of the powders, which is less than 40% of that of solid silicon, causes poor crucible loading factor and unacceptable low productivity in casting processes;
- Significant amount of silicon oxide, which is present on the powder surface, decreases the electrical conductivity and requires overheating for melting. Poor ingot quality is obtained in case silicon oxide is not properly removed before the crystallization step.

GARBO has developed a binder-assisted compacting densification method to produce porous bodies of silicon powders of relatively high density and mechanical stiffness. The process utilizes a sol-gel technique in which the silicon powders are mixed with a solution containing a silane precursor, water and a solvent to obtain the dense slurry which is subsequently shaped into bricks and granules of desired size. The combination of bricks and granules allows maximizing the crucible charge density in the melting and crystallization step. Mechanical stiffness and densification is achieved through formation of a Si-O-Si rigid network.

The input

The inlet material in the silicon recycling plant consists in a mixture of silicon kerf powder with residual coolant used during FAS operations as shown in Figure 1. The material is in form of a sludge and/or filtration cake. The typical composition of the incoming silicon kerf is as follows:

- Silicon (Si) 59.8%
- Silicon Oxide (SiO2) 5.2%
- Glycol (coolant) 35%
- diverse Metals 0.02%

Figure 1: Incoming kerf loss

The material comes from a European-based silicon wafer producer using a glycol-based coolant. The silicon oxide content derives from oxidation of the Si kerf in contact with the water and oxygen dissolved in the coolant. Given the extremely small particle size (well below 1 micron) the kerf is very reactive and even small concentration of dissolved water and oxygen can form substantial amount of silicon oxide on the particle surface. Beside coolant and silicon oxide, further contamination on the silicon is caused by metals introduced by the cutting tool, typically Nickel from diamond wire coating.

The process

The recycling process is divided into the following different process steps:

- Si kerf/coolant separation

The first step of the recycling process is the separation of the silicon particles from the liquid and the recycling of the liquid (which is mandatory for solvent based coolant). This step is typically carried out at customer site via filtration or centrifugation. The resulting material is a sludge/ filtration cake.

- Cleaning

The first step of the recycling process performed at GARBO's premises is the cleaning treatment aimed at removing all contaminants from the surface of the silicon particles. Typical impurities are various organic compounds arising from the coolant, metal impurities arising from the steel wire and steel parts of the saw and silicon oxide arising from oxidation of the silicon particles as seen in the composition of the incoming Si kerf.

- Compacting

Here, the clean silicon kerf cake is mixed with the methyl silicate binder and water according to the compacting recipe and fed to a roller compactor. The output of the compacting section consists in ovoid-shaped silicon briquettes (see Figure 2).

- Drying

The drying of the compacts was performed in an inert atmosphere (typically under 50-100 mbar vacuum) in order to remove the solvent. The solvent is evaporated by a controlled thermal treatment, condensed in a reflux column and recovered in the process. Dried briquettes are obtained with good mechanical properties for crystallization experiments.

- Sintering and oxygen removal

High temperature thermal treatments have been carried out in order to remove the oxygen content from the surface of the compacts. The reaction occurs at temperatures above

1200°C and results in a formation of silicon monoxide gas. Depending on the process parameters, the oxygen content can be decreased by a factor of 10…20.

- Solvent reclaiming

The filtrate stream, which is an output of the cleaning section, needs to be treated in order to neutralize the acidity from hexafluorosilicic acid (H_2SiF_6) and hydrochloric acid (HCl) and to reclaim the glycol to be used in a closed-loop mode in the process. The neutralization reactions occur by properly dosing sodium hydroxide solution.

Some facilities of the pilot plant and the achieved silicon briquettes are presented in Figure 2. The sintering process was included as additional step into the recycling process. During the course of the SIKELOR project, thinner diamond wires have been used in FAS production by GARBO's FAS partner, with core wire diameter shrinking from original 120 micron to the current size of 80 micron. Diamond wires having a size of 60 microns are presently at the experimental stage for FAS production. Concurrently, the average size of the silicon kerf particles has been reduced from 0.36 micron (120 micron thick wire) to 0.21 micron (80 micron thick wire), thus yielding a 71% increase of the specific surface area and a consequent increase of the native oxide content. This incremented oxygen content introduced new challenges to the project since only a limited amount of oxygen in the silicon charge can be handled during melting and crystallization process for multi-crystalline ingot growth. For that purpose, high temperature thermal treatments have been tested in order to reduce the oxygen content.

(a) (b)

(c) (d)

Figure 2: Pictures of the chemical pilot plant available at GARBO: (a) cleaning section, (b) briquetting facility, (c) drying furnace, (d) silicon briquettes.

Before starting the recycling process, every section of the pilot plant has undergone a debug program to check its functionality from the electrical and mechanical point of view. The cleaning section has been started with a water test to specify the filtration parameters. The first charge of silicon kerf loaded in the cleaning line has been treated with HCl only in order to optimize the filtration parameters such as the cycle time, the silicon cake thickness and cake residual moisture. Because the fine silicon kerf powder is highly reactive, optimization of parameters like flow rate and stirring velocity of the suspension in the reactor has been carried out on condition that the temperature is tightly controlled at 20°C and hot spots are avoided. The washing step of the cake after the acid treatment has been performed until a neutral pH of the filtrate stream is obtained. A sample of treated Silicon cake is withdrawn at the end of the washing step for analysis in order to verify that residual impurities like metals, organics, oxygen level, and total moisture content are compliant to specifications. Finally, the start-up of the remaining plant sections has been accomplished smoothly without problems. Samples of silicon compacts are taken from every batch after sintering to perform quality control on the final material. Ramp-up to full-scale production has taken approximately one month and continuous operation has been put in place based on 2 or 3 shifts per day.
The pilot plant has a capacity of ca. 7 kg of recycled silicon per day based on 24 hours per day operation. The plant capacity is dictated by the cleaning process as limiting step. The recycled silicon feedstock was delivered to the partner University of Padova (UNIPD) and used there as starting material for the first crystallization experiments performed in April/May 2016.

The output
The outlet material from the plant is a recycled silicon feedstock with 5.5N metal purity in form of a compacted powder (briquettes) having a density of approximately 1.6 g/cm^3. Typical composition of the recycled silicon kerf is listed below:

- Silicon (Si) 96%
- Silican oxide 4%
- Metals < 0.05%

The residual silicon oxide content originates from the native oxide formation on the sub-micron sized powder due to the exposure of the porous silicon compacts to the air. This amount of silicon oxide represents the natural oxidation of the material and cannot be prevented in an oxygen containing atmosphere. The metal content was reduced down to part per million level in order to satisfy solar application requirements.

Quality control
Comparative analyses have been performed by GARBO in order to assess the purity of the refined GARBO kerf in relation to high purity Poly-silicon and UMG grade Silicon from ELKEM. The results are reported in the Table 1 below.

Alkali and alkali earth metals have been detected in the GARBO kerf mainly arising from the ubiquitous contamination from the environment on the nanosized material (no clean room available for metal digestion preparation). Moreover, GARBO kerf contains higher transition metals compared to ELKEM Silicon. On the other hand, ELKEM Si shows a higher content of B and P dopants. Specifically, the B level is very dangerous and may lead to light induced degradation effects due to boron-oxygen complexes. Additionally, the simultaneous presence of B and P in ELKEM Silicon affects the resistivity profile. This fact requires specific counter-measures for keeping a flat resistivity along the resulting ingot. Lastly, UMG Silicon is sold at a price that is about 15% (max. 20%) lower than that of virgin poly-Silicon while the

target price of recycled Si kerf is much more competitive being 50% of the price of standard polysilicon.

	Si clean kerf GARBO ppb w	High purity poly-Si [6] ppb w	UMG-Si ELKEM [7] ppb w
Al	80	1,22	< 150
B	< 10	10	260
Ca	120	11,9	< 3000
Cr	80	0,04	na
Cu	90	< 0,4	1
Fe	520	< 0,44	< 80
K	50	< 1,47	< 0,5
Mn	< 10	< 0,02	na
Na	< 10	< 0,16	0,3
Ni	730	< 0,16	1
Zn	< 10	0,18	< 0,02
Ti	120	< 0,01	< 100
P	120	11,1	680

Table 1: Results of chemical analysis comparing the GARBO kerf with commercially available feedstock

Cost assessment

The key economics of an industrial plant for the recycling of FAS kerf utilizing the above described process and located inside GARBO's facility have been evaluated.

2000 MT/year Silicon plant - Cash cost		
DIRECT LABOUR		**1.344.000**
PRODUCTION STAFF & SERVICES TO PRODUCTION		**290.800**
LABORATORY (labour, auxiliary)		**138.000**
DIRECT MATERIAL COST		**1.650.000**
Raw Si kerf purchase	0	
Chemicals & Process Gases & Auxiliaries	1.500.000	
Packaging	150.000	
MAINTENANCE & SPARE PARTS		**406.500**
FREIGHT COST IN		**276.000**
FREIGHT COST OUT		**300.000**
UTILITIES		**2.250.000**
Industrial Electricity	2.100.000	
Natural Gas	120.000	
Solid disposal	30.000	
OTHER PRODUCTION COSTS		**50.000**
Miscellaneous	50.000	
TOTAL INDUSTRIAL COSTS		**6.705.300**
OVERHEAD		**532.500**
Office manager	50.000	
Admistration & Accounting & Sales	112.500	
Insurance (All risks)	70.000	
Marketing cost	60.000	
Plant security	40.000	
Technical Consulting	100.000	
Legal & Fiscal Consulting	50.000	
Information Technology (website, PC maintenance, ADSL…)	20.000	
Miscellaneous (fixed line, stationery, others)	30.000	
TOTAL OVERHEAD		**532.500**
FINANCIAL COSTS (bank account)		**413.038**
TOTAL CASH COST		**7.650.838**
UNITARY CASH COST		**3,83**

Table 2: Costs of the pilot plant for kerf loss cleaning & compaction (in €/kg) estimated by GARBO

A basic engineering study was carried out to dimension the relevant equipment and to calculate mass and energy balances to the extent needed for a cost evaluation with an accuracy of about ± 30%. In order to achieve the best possible accuracy, GARBO relies on its experience and procurement data as well as on budgetary quotations from suppliers. The following assumptions are taken:

- Plant capacity = 2000 MT/year of recycled silicon.
- Plant uptime > 90%, with operation 24h/day, 7 days per week.
- Sintering and Oxygen removal step: included.
- Recycling yield > 90% calculated on the silicon content of the incoming kerf.
- Recycled silicon sold in a closed loop to original wafer producers.

The incoming material to be processed comes from different wafer FAS manufacturers with whom GARBO has already business relationships for FAS coolant recovery. These customers are interested in silicon kerf reclaiming. The adopted business model foresees to offer the silicon reclaim service to the customer in a closed-loop mode similarly to the LAS slurry recycling activity: FAS wafer manufacturer sends to GARBO the Si kerf waste for processing

and receives back the reclaimed material at defined quality specification, recycling yield and price. The price for recycled Silicon is set to 50% the price of standard polysilicon, which is equal to 14 EUR/kg (April 2016). Therefore, the unitary costs for silicon kerf recycling are expected to be well below 7 EUR/kg in order to guarantee business profitability.
Table 2 (see previous page) reports the cash cost calculation made on an annual basis for the plant producing unitary cash costs of 3.83 EUR/kg. Taking the CAPEX into account the total unitary costs for a 2000 MT/year silicon plant add up to 4.39 EUR/kg for the recycled silicon (see D4.5 for more details). These costs are well below the target price of the recycled feedstock thus making the business of the kerf loss recovery highly attractive.

II) Numerical and experimental modelling

The SIKELOR project aims at obtaining clean silicon material by removing impurity particles (mainly silicon carbide, SiC) from the initially contaminated material using the electromagnetic separation technique and electromagnetic mixing applied during crystallization of liquid silicon. Electromagnetic separation is one of the most promising methods for inclusion removal, which is based on the works done by Leenov and Kolin [8] and Marty and Alemany [9]. Various methods have been proposed to generate electromagnetic forces in liquid metals: simultaneous imposition of direct current and stationary magnetic field; imposition of alternating current; simultaneous imposition of alternating current and AC magnetic field; or imposition of AC magnetic fields (alternating and/or traveling magnetic fields). In spite of many researches on electromagnetic separation, the effect of induced flow of liquid metal on the separation efficiency has not been clarified yet. Within SIKELOR we followed the approach of using AC magnetic fields for separation. Applying a high-frequent alternating field on an electrically conducting fluid induces electric currents and a pressure force on the fluid. SiC particles are electrically non-conducting. Suspended in the conducting silicon melt, these particles pose an obstacle for any electric current. The redistribution of the electric current exerts an additional force on these particles. This magneto-electrophoretic Leenov-Kolin force (LKF) provides an efficient way to separate the particles from the melt. In the field of metallurgy, such electromagnetic separation of particles from a molten metal is an emerging and promising method for the production of ultra-clean metal. There are a number of previous publications considering the origin of particles, their transport, incorporation and removal during the directional solidification of silicon material. However, the underlying effects are far from being completely understood. The necessity of the intense modelling activities in the project is obvious. Numerical modelling of fluid flow and transport processes within SIKELOR was performed by UNIG. The numerical part was supported by experimental modelling at HZDR. In particular, the isothermal model experiments using the eutectic alloy GaInSn provided data of the flow structure generated by an alternating magnetic field (AMF) for validation of the numerical codes. It should be noted that all previous studies that provided reliable data about electromagnetic stirring and electromagnetic separation generated by an AMF are rather far from any industrial practice. Especially, experimental data with respect to the AMF-driven flow structure are fragmentary and inconsistent for the parameter range of high shielding parameters.

Numerical codes

The previously existing axisymmetric 2d SPHINX code at UNIG was applied and adapted for the needs in the SIKELOR project. This software is based on the pseudo-spectral method. Furthermore, a full 3D code was developed in the course of the project. A benchmark test of both approaches was done based on a setup of liquid silicon in a graphite crucible of both circular geometry and rectangular cross-section, respectively, and a coil of circular windings. The comparison demonstrates that the axisymmetric solution is predicting quantitatively very

similar electromagnetic field distribution, except in the side corner regions where the rectangular shape imposes some dissimilarity. The axisymmetric numerical solution permits much faster and more flexible approach, enabling to follow the dynamic solidification front motion, free surface deformation and perturbation, the Lagrangian tracking of the impurity particles over large time intervals. The 2D solution gives a possibility to investigate quickly large number of the AC magnetic field versions and even their combinations, like the travelling field and single phase fields of wide range of frequencies.
The newly modified version of the SPHINX code includes further features such as the travelling magnetic field in addition to the single-phase field, a deformable free surface, the effect of the stochastic forcing and the added drag force on spherical particles. The 3D model has the capability to calculate the electromagnetic field, the resulting stirring force (average and time-dependent), Joule heating, liquid flow and solidification in square crucibles or any 3D geometry. It was successfully applied to model the complex geometry of the Padua *i*DSS furnace. The in-house multi-physics computational environment Physica3g can be used for fully coupled electromagnetic-thermo-fluid simulations with solidification and existing particle tracking routines as required.

Model experiment

The sense of physical modelling is to gain an inside into phenomena which are not measureable inside industrially relevant high-temperature melts. An optimal set of magnetic field and process parameters has to be identified in order to achieve an efficient separation of particles. A particular challenge is the control of the fluid flow. On one hand, the electromagnetically driven convection has to carry the particles from the bulk towards the side wall where the maximum LKF is expected. On the other hand, a too intensive electromagnetic stirring bears the risk of withdrawing the particles already collected in the separation zone. Therefore, the physical modelling was exclusively focused on the investigation of the flow pattern driven by an AMF.
Two versions of the experimental setup were realized. The first configuration is shown in Figure 3 and concerns the flow in a cylindrical container. The eutectic alloy $Ga_{68}In_{20}Sn_{12}$ which is liquid at room temperature was used as model fluid. The Ultrasound Doppler Velocimetry (UDV) was applied for flow measurements [10]. The coil system in this first setup is cylindrical, whereas those systems in the Demonstrators are of quadratic shape. While the different coil shapes are expected to evoke comparable effects, the numerical simulations have shown deviations of the magnetic field in the corners between a circular and a rectangular melt volume. These deviations cannot be regarded as negligible and may have a distinct effect on the fluid flow. Another significant limitation is the maximum achievable field strength in the upper frequency range. The experimental setup was modified in the second project period in order to provide an experimental hardware capable of modelling the flow in the Demonstrators on a reasonable scale. The setup involves now a coil system of quadratic shape. The partner EAAT has built a power supply for this new coil which is capable of producing magnetic field strengths an order of magnitude higher as in the first variant. As a consequence, the flow measurements can be extended far into the turbulent range. Rectangular and cylindrical fluid containers are available which can be exchanged between both systems. The new experiments are of a size corresponding to G1, and can be performed up to a shielding parameter as high as it is in the Demonstrator. Even crucible sizes as used in the *i*DSS furnace at the UNIPD would easily fit into the magnetic field system. The new setup is displayed in Figure 4.

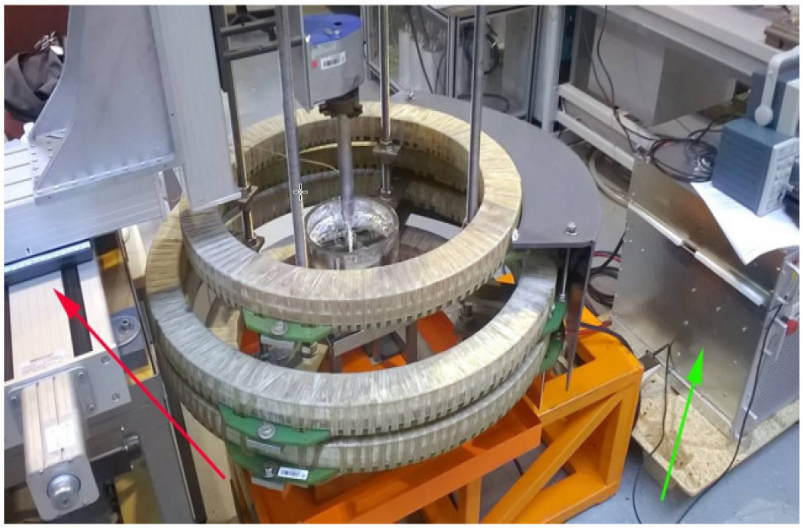

Figure 3: Photograph showing the first experimental setup utilized for flow measurements in a cylinder driven by an alternating magnetic field

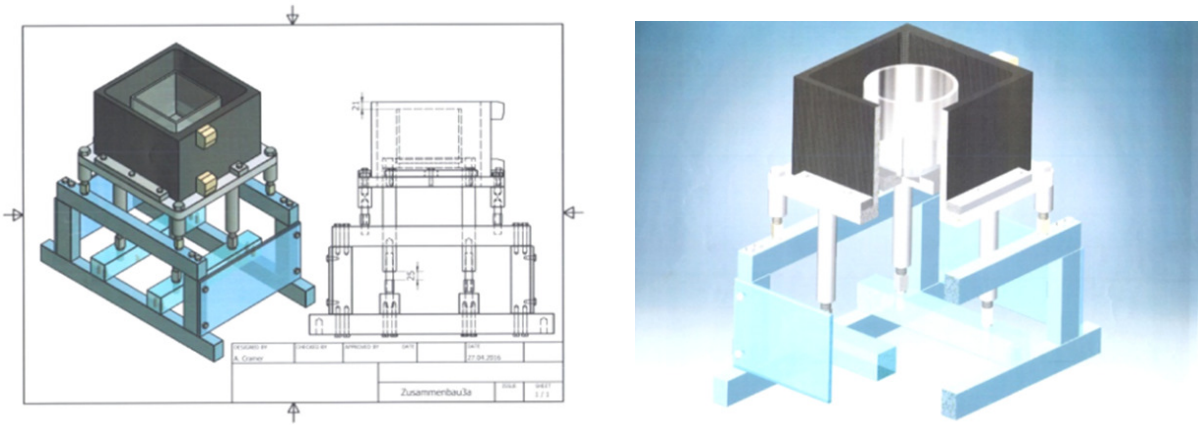

Figure 4: Technical drawings of the modified setup of model experiments at HZDR

Validation of the numerical code

As a first step in the work program on numerical modelling a reproduction of numerical and experimental data previously published in the literature [11-15] was done. Especially, the quasi-benchmark against the experimental data by Kadkhodabeigi et al. [11] was important since that experiment is the only successful demonstration of separation in silicon so far. Figure 5 demonstrates that the numerical simulations were able to reproduce the literature data. On this basis of these data a first up-scaling towards the SIKELOR Demonstrator was done. Here, it became obvious that the magnetic field frequencies for achieving separation are higher as expected at the beginning of the project. This finding has serious consequences on the construction of the Demonstrator, in particular, the hot zone.

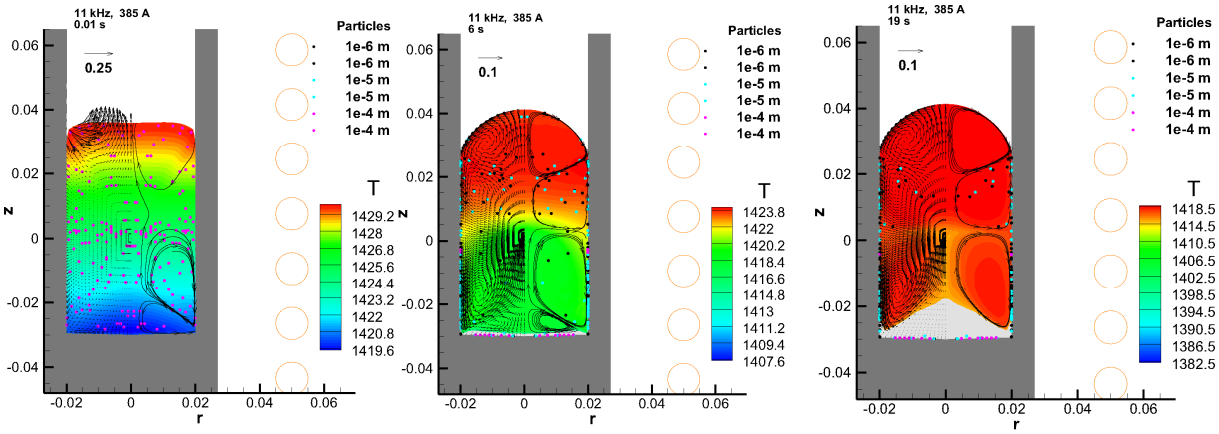

Figure 5: Numerical calculation of the particle separation for the experiment in [11]

In a further step, the numerical software developed at UNIG was applied to simulate the GaInSn experiment performed at HZDR. The measurements deliver a valuable data base for verifying the numerical models and reveal new previously unexpected features of the AMF-driven flow. Against all expectations to obtain a steady double vortex in such a weak flow a multi-layer arrangement of vortices was observed. In general, both the position and the size of the respective vortices are subject to periodic variations. Exemplary results presented in Figure 6 demonstrate the evolution of profiles of the vertical velocity parallel to the side walls of the fluid container. These data sets were recorded at different frequencies of the AMF resulting in different shielding parameters of $S = 2\pi\mu\sigma f R$ (where μ, σ and f stand for the magnetic permeability, electrical conductivity and the magnetic field frequency). While the well-known double vortex occurs at moderate values of $S = 5$, a sandwich structure of four vortices can be observed at $S = 50$.

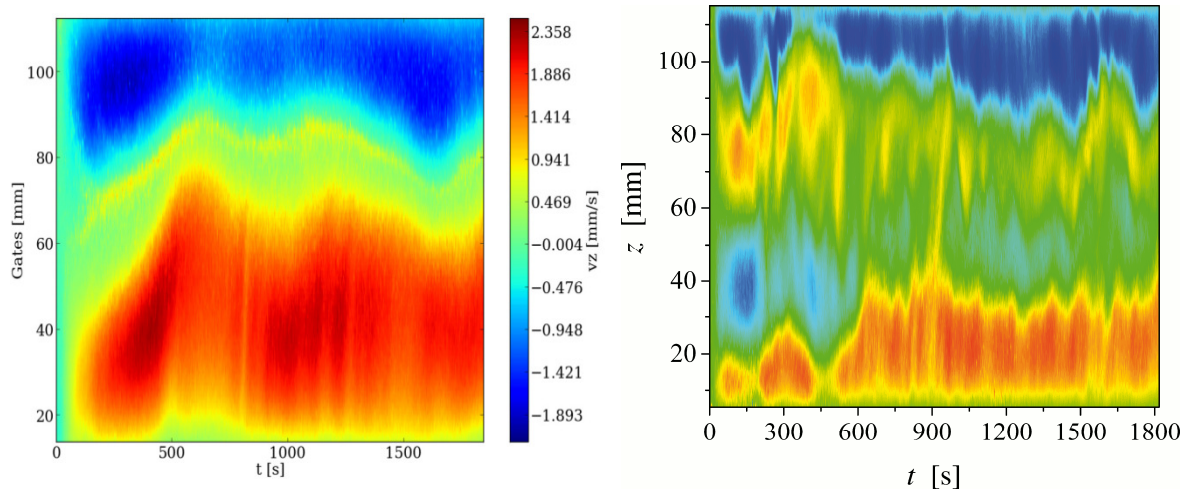

Figure 6: Spatio-temporal flow structures of the vertical velocity component along the side walls of the fluid vessel recorded at a shielding parameter of S = 5 (left) and S = 50 (right), respectively.

The fluctuating features of the toroidal vortex structures are reproduced by the numerical solution (a corresponding arrangement of a four vortex structure is shown in Figure 7), indicating the origin of this in the non-linear flow instability and a transition to new periodically oscillating states. Despite the limited induction, the results obtained could be even described as outstanding or striking. Further analysis was performed to quantify these findings and to transfer the results to the real application of the silicon melt inside a larger scale crucible.

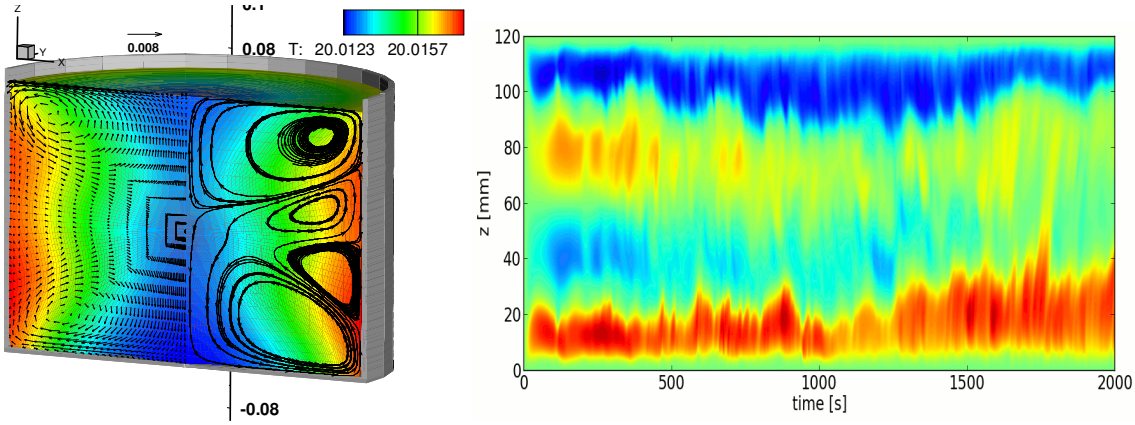

Figure 7: Time-averaged velocity field in liquid GaInSn and temperature field for S=50 (left), spatio-temporal flow structure of the vertical velocity component along the side walls of the fluid vessel recorded at S = 50

Simulation of Demonstrator I

The objective of the 3D modelling of Demonstrator I was to predict the ability of this arrangement of coils to induce an adequate stirring of the melt as well as to capture impurities. Figure 8 shows the representation of the side coils in the model. The arrangement consists of 6 symmetric closed square windings made of graphite where each turn has a rectangular cross-section. The mesh of the computational model in the quarter-domain is also visible.

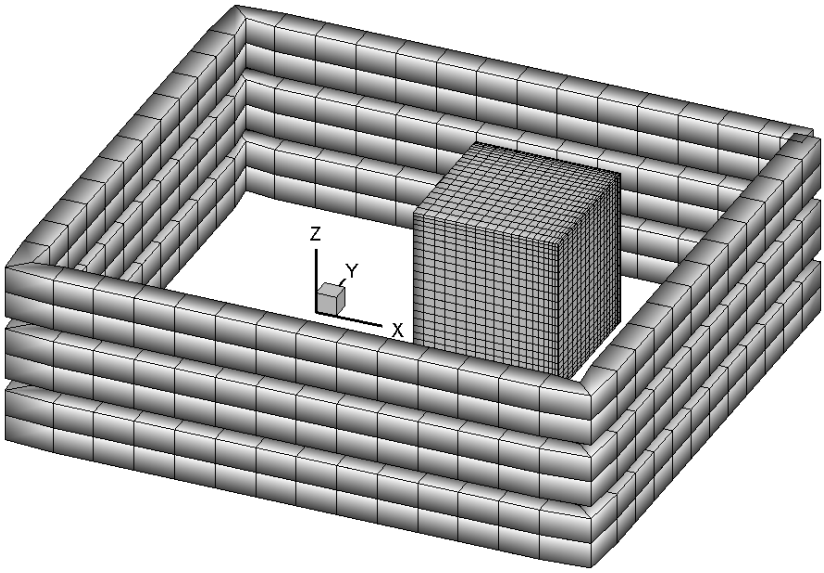

Figure 8: Computational mesh and symmetrical coils of Demonstrator I

Two sets of operational parameters were modelled:

- 100 Hz, AC current of 768 A with a phase-shift of 120^{o} in the 3 side coils producing a travelling magnetic field (TMF), whose Lorentz force is directed upwards, and
- a single phase current through the topmost coil only.

The corresponding flow patterns in the molten silicon are depicted in Figure 9 (half of vertical cross-sections through the middle of the liquid volume). The flow structure appears to be completely different in the two cases: the TMF produces a double-roll pattern where the liquid rises at the ‘y’ ends and sinks in the middle of the actual volume while the single-coil flow is dominated by jet-like streams along the upper edges of the liquid volume which are exposed to the strongest magnetic field. The maximum liquid velocity is higher in the single-phase case.

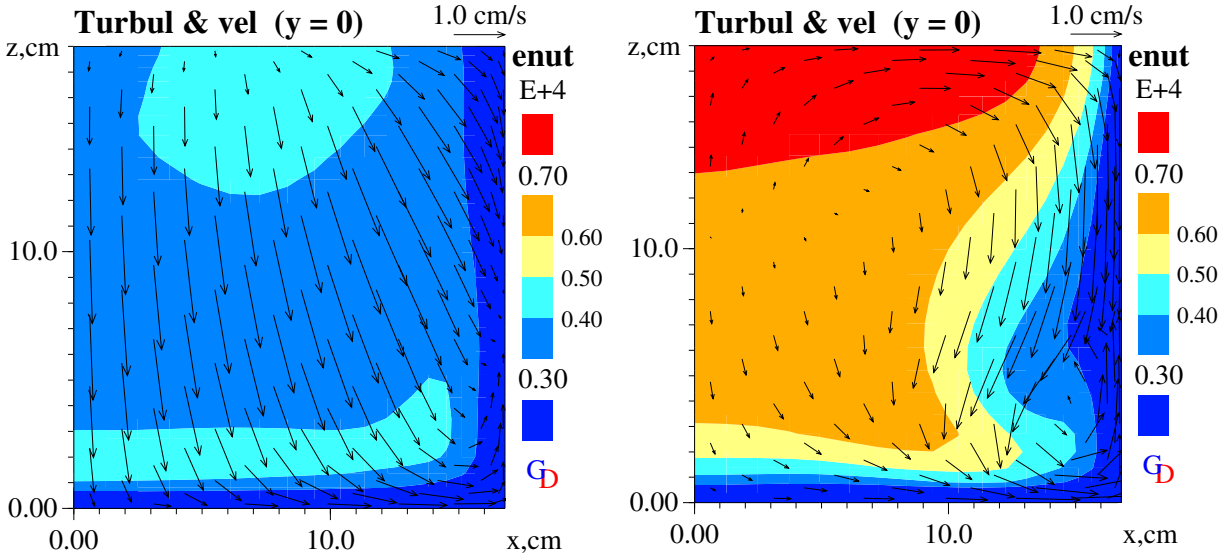

Figure 9: Liquid velocities (vectors) and turbulent viscosity (color) for the two cases: TMF (left) and top coil (right)

The non-conducting inclusion particles are subjected to fluid drag, Leenov-Kolin force and gravity forces. The fluid drag depends on the velocity difference between the liquid and the particle and on the particle frontal area determined by the particle size. In order to obtain a conservative estimate of the influence of the fluid drag on particles in different locations within the liquid volume, the particle velocity is assumed to be zero in the calculation of the total force, i.e. the maximum possible value of this drag is used for the estimates. The Leenov-Kolin force acting on electrically non-conducting particles depends on the local strength of the electromagnetic field (magnetic induction and current density) and, ultimately, on the driving coil current. The gravity force is proportional to the density difference between the particle and liquid silicon; for this study SiC spherical particles with density 3210 kg/m^3 were used. For a better assessment in which direction the particles will be pushed at each cell location, a 'dot product' criterion is constructed by vector multiplication of the fluid drag force and the Leenov-Kolin force and subsequent division by the weight of the particle 'Gp'. The results for the case without solidification, i.e. the whole volume is filled by liquid silicon, are presented in Figure 10. The arrows in both parts of Figure 10 represent the non-dimensional particle resultant force vectors, i.e. the force magnitudes are divided by the weight of the particle 'Gp' corresponding to 50 µm particles in this case. The maps are drawn for a vertical section near the crucible wall. We know that the Leenov-Kolin force near the wall is non-zero and directed towards the wall, therefore the dot product shows the likelihood of particles of the given size being retained at the wall. At positions, where the dot product 'dotp' gives positive values, the fluid drag force is directed towards the wall and promotes a particle motion in that direction. With decreasing distance from the wall the particle behaviour becomes more and more determined by the dramatically increasing Leenov-Kolin force. The particles enter the fluid-flow boundary layer where both fluid velocity and turbulence decrease rapidly. Here, the Leenov-Kolin force becomes fully dominant. It can be assumed that the particles are retained in this region while the solidification front arrives.

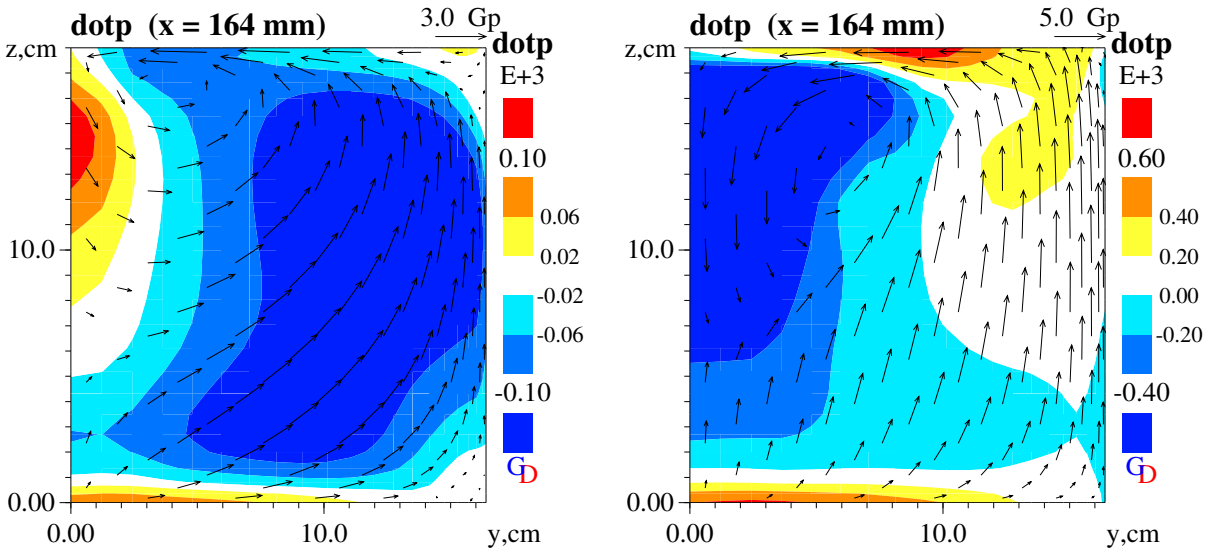

Figure 10: Dot product and resultant force maps for 50 µm particles in Demonstrator I
left: travelling magnetic field; *right*: single phase

The observed values of the separation criterion 'dotp' are very low and predominantly negative in the 'x'-ends (the ends of the slightly longer side) of the crucible. Figure 11 shows the other two sides of the liquid volume (the 'y'-ends of the shorter side) and reveals a similar force distribution there. The single-phase case (on the right) provides slightly better results although the positive 'dotp' values are rather small. Therefore, in terms of a significant separation the calculations disclose that the installation of 3 graphite coils does not provide an advantage compared to the operation of the single coil at the top of the liquid volume at the same current. Thus, our investigations yield a preference of the single-phase option. It would be cheaper and generates more vigorous mixing and has a small chance of inclusion particle separation on two of the crucible side walls. All in all, the magnetic field configuration in Demonstrator does not provide good prospects for achieving particle separation.

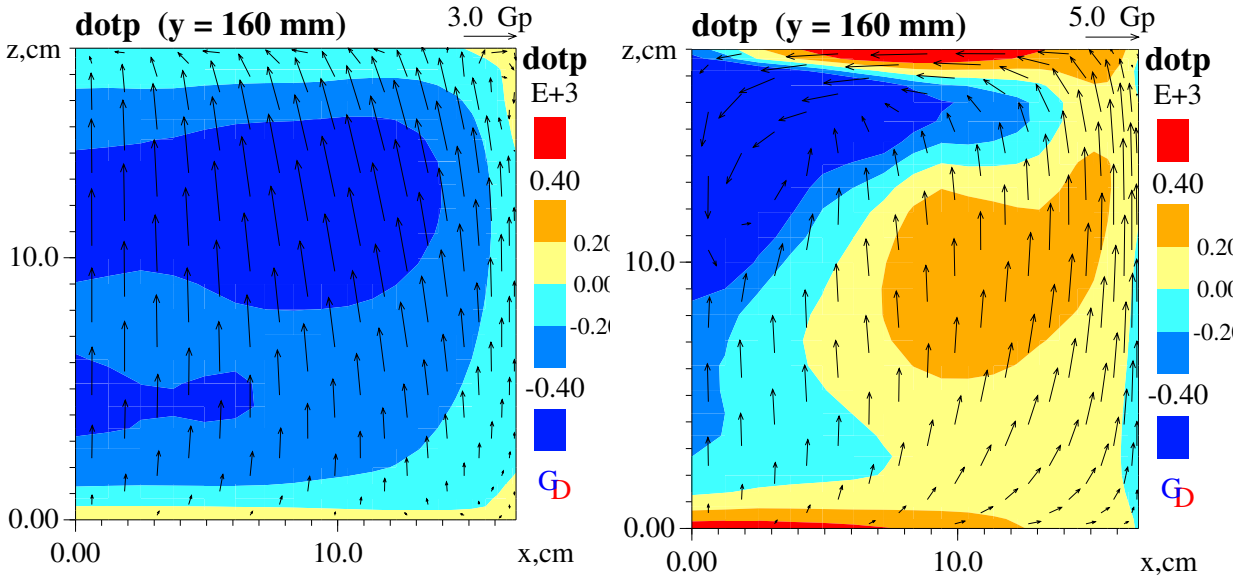

Figure 11: Dot product and resultant force maps for 50 µm particles in 'y' ends:
left: travelling magnetic field; *right*: single phase

Simulation of Demonstrator II – G2.5 experiment

A schematic drawing of the setup and the computational scheme are shown in Figure 12. The inside dimension of the square crucible is 410 mm. The height of the volume of liquid Si is assumed to be 230 mm.

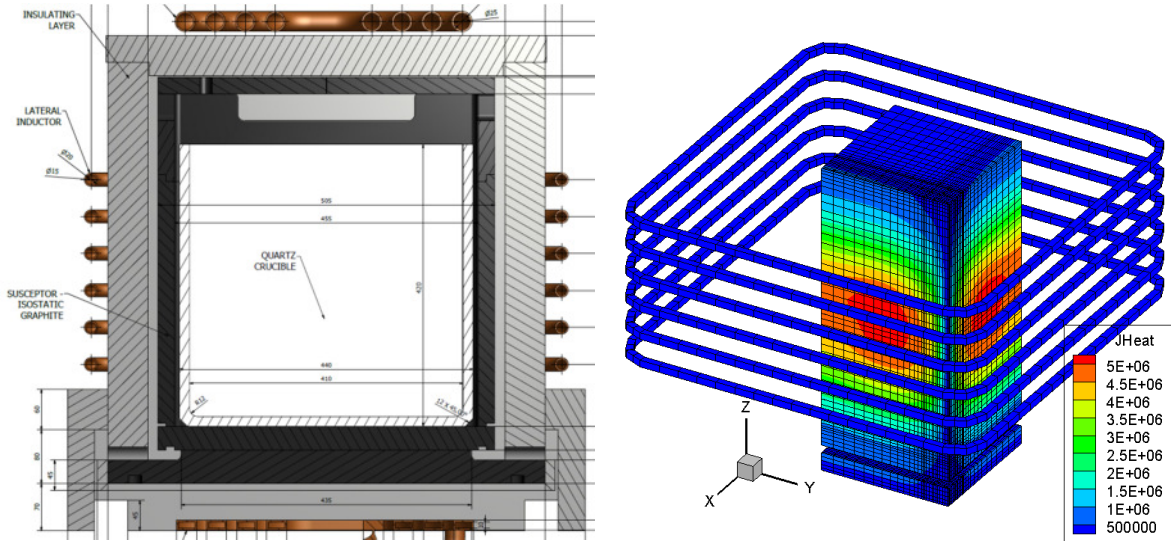

Figure 12: Schematic drawing of the *i*DSS furnace with G2.5 crucible (left), computational mesh, Joule heating and symmetrical coils of the *i*DSS G2.5 model (right)

The operational parameters modelled were identical with those adjusted for the experiments at the University of Padua with the G2.5 crucible: AC current of 1300 A, single phase through all 6 side coils at 2300 Hz and no current in the bottom or top coils. Figure 13 demonstrates that the 3-dimensional structure of the flow is dominated by a jet-like stream pushed inwards and downwards from the upper corners of the liquid volume. Figure 13 also contains maps of the resultant forces on the particles and the dot product maps. Again the snapshots were made before the solidification starts. The arrows in Figure 13 represent the resultant non-dimensional particle force vectors, i.e. the force magnitudes are divided by the weight of the particle 'Gp' corresponding to 50 µm particle in this case.

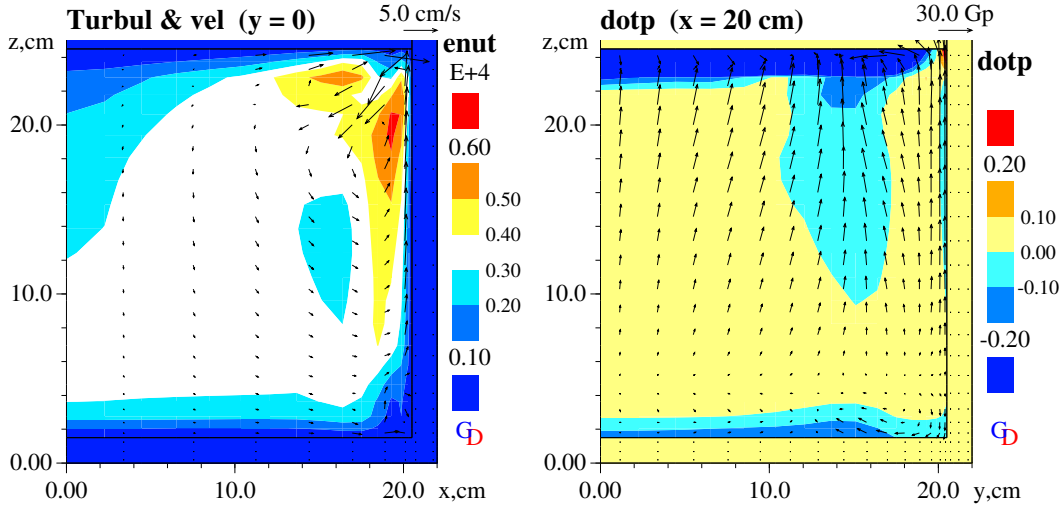

Figure 13: Liquid velocity vectors and turbulence effective viscosity (left) and dot-product criterion (right) for 50 µm particles in the *i*DSS G2.5 experiment

The observed particle force distribution remains consistent during the ingot growth – wide areas show a positive dot product. Thus, the computed 3-dimensional model predictions of the behaviour of SiC particles in the *i*DSS furnace with the G2.5 crucible at 1.3 kA, 2.3 kHz indicate a significant separation effect and retention of non-conducting particles at the wall.

Simulation of Demonstrator II – G1 experiment

Figure 14 shows the configuration of the G1 experiment including the 12 side coils represented in the model as symmetric closed square wires (without the contact leads). The mesh of the computational model quarter-domain is also visible.

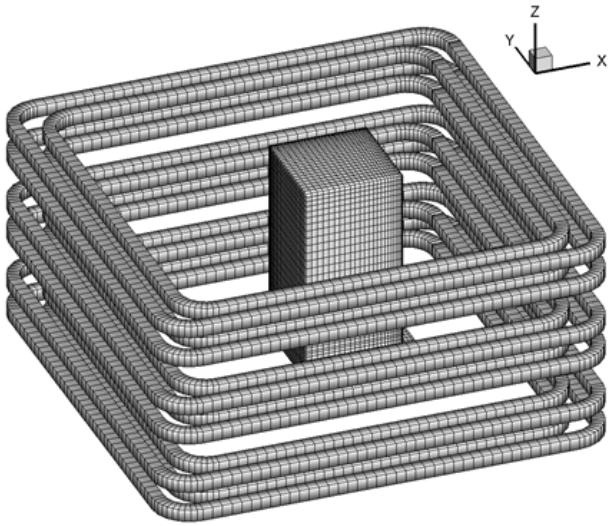

Figure 14: Computational mesh and symmetrical coils of the *i*DSS G1 model

Several sets of operational parameters were modelled taking into account a single phase AC current for all 12 symmetric side coils. Here, we compare the following cases:

- case 1: 1000 A at 4 kHz, and
- case 2: 350 A at 2 kHz.

Again, the purpose of the modelling is to analyze the forces acting on inclusion particles and to predict the capability of the magnetic system in Demonstrator II to purify the silicon by holding the particles on the crucible walls until they are captured by the solidification front.

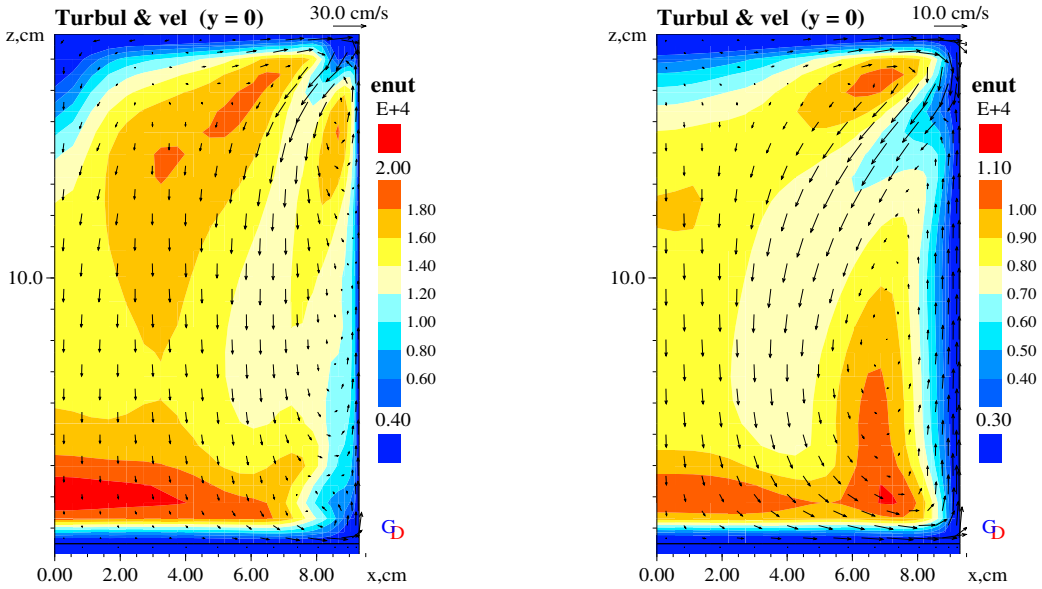

Figure 15: Liquid velocities and turbulent viscosity for examined G1 cases: *left*: case1, 1 kA, 4 kHz; *right*: case 2, 0.35 kA, 2 kHz

The flow structures presented in Figure 15 are dominated by jet-like streams pushed inwards and downwards from the upper edges of the liquid volume. The maximum liquid velocity in case 1 is 3 times higher than in case 2 while the difference in the extent of turbulent mixing

(measured by the effective turbulent viscosity 'enut') is about two times. Nevertheless, even the weaker case 2 exhibits sufficient, even rather vigorous mixing throughout the liquid volume. Figure 16 presents the results of the resultant forces on the particles (in terms of the so-called 'dot product' criterion, see previous section) for both cases of magnetic fields. It becomes obvious that the dot product exhibits significant positive values over wide areas. This gives a positive forecast with respect to a successful separation of non-conducting inclusions in the near-wall regions. Because of the very high values near the bottom of the crucible we can expect an efficient entrapment of particles in this domain.

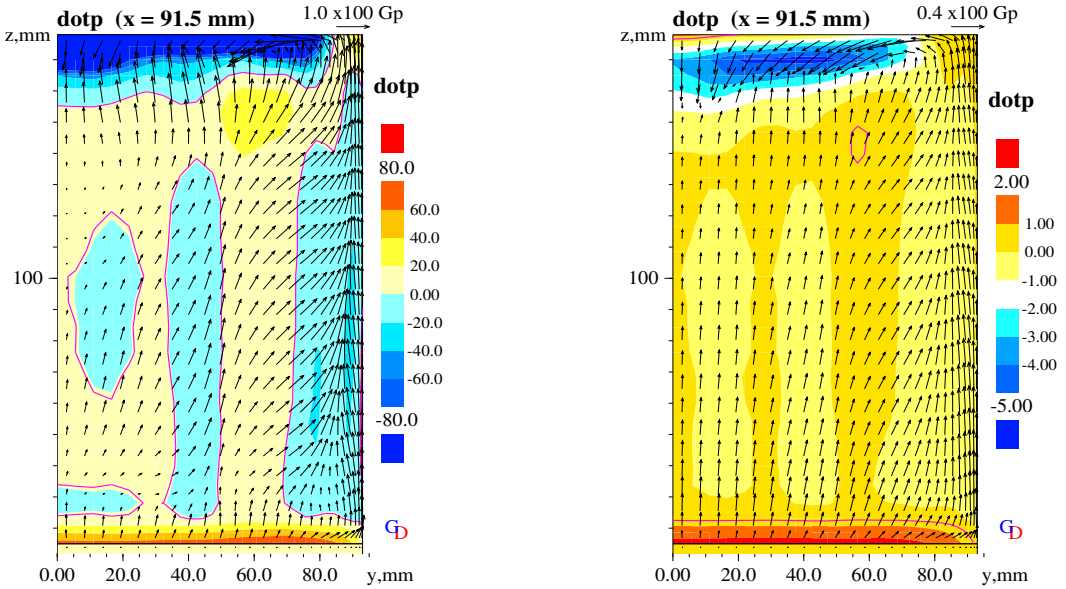

Figure 16: Dot product and resultant force maps for 50 µm particles in G1 model: *left*: 1 kA, 4 kHz; *right*: 0.35 kA, 2 kHz

Calculations of the resultant particle distribution were done in the axisymmetric configuration starting from a random uniform distribution. The different particle concentrations at later stages results from the interplay between an intensive electromagnetic stirring and the Leenov-Kolin force whose efficiency becomes largest near the wall. Exemplary results are presented in Figure 17 for case 1 considering SiC particle sizes of 1, 10 and 100 µm. The particles recirculate in the toroidal loops many times. This snapshot demonstrates that the particle capturing in the skin-layer region starts almost immediately, where the high force magnitude ensures particle retention. An additional fraction of particles is accumulated at the bottom of the solidified material.

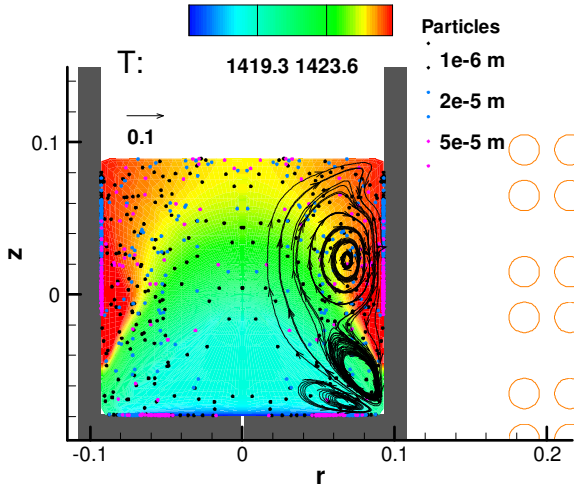

Figure 17: Instantaneous streamlines and the Lagrangian particle tracking (1 kA, 4kHz)

In summary, it can be concluded that the dynamic particle tracking algorithm demonstrates the difference between the particle paths and the instantaneous streamlines. The fully developed turbulent flow affects the particle retention in the skin-layer via the turbulent fluctuation of flow velocity and the chaotic drag variation. However, the high magnitude of the electromagnetic force in the G1 configuration ensures trapping of particles in the side skin-layer and at the bottom of the ingot.

III) Implementation of the Demonstrator II and crystallization experiments

The Demonstrator II was built within SIKELOR on the basis of the *i*DSS furnace installed in the laboratory of UNIPD. The *induction* Directional Solidification System (*i*DSS-unipd) is a prototype of induction vacuum furnace designed for melting and directional solidification of silicon. Quartz crucibles with a maximum load of 120 kg can be installed inside this furnace. The furnace is equipped with three independent inductors, each one fed by a specific generator (60 kW, 2 – 10 kHz). Figure 18 shows a schematic drawing of the Demonstrator II.

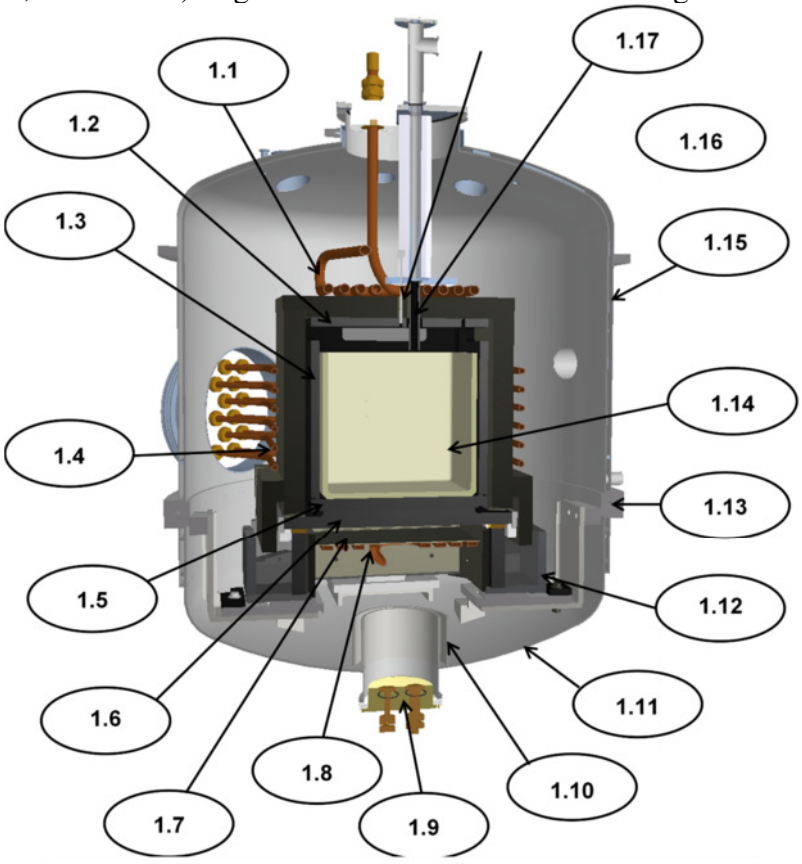

Figure 18: Schematic drawing of Demonstrator II at UNIPD

The main parts of the furnace are (see also deliverable D8.4 for detailed description):

- Stainless steel vacuum chamber
- Mechanical structure of the vacuum chamber and its control unit (PLC for mechanical movements)

- Electrical power system, that comprises: power connections and switches, auto-transformer, 3 parallel resonant generators, 3 groups of inductors
- Isostatic and felt graphite in the hot-zone
- Main Control System based on a Siemens PLC fed by an UPS
- Vacuum pumps
- Water pumps and hydraulic cooling system for generators, capacitor banks, inductors and walls of the vacuum chamber
- Cooling system, based on 2 chillers
- Argon flow supply and control system
- Sensors and probes for measurements

Two different experiments were realized in the Demonstrator II considering the G2.5 and the G1 geometry, respectively.

G2.5 experiment

The core of furnace is the hot zone, which is located into a steel vacuum chamber made of a double layer of stainless steel (see Figure 19(a)). The heating system is realized by three independent inductors (Figure 19(b)), which are made of copper and must be water cooled with forced flux. The graphite box in Figure 19(c), that surrounds the silica crucible where the silicon is melted, works as susceptor for the side inductor and it must guarantee the mechanical stability to the silica crucible that becomes soft at high temperatures. In the experimental test, we used a box made with a monolithic block of isostatic graphite. This solution offers higher safety in case of failure.

(a)

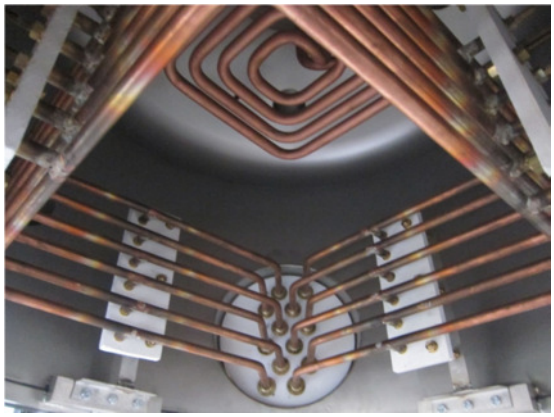

(b)

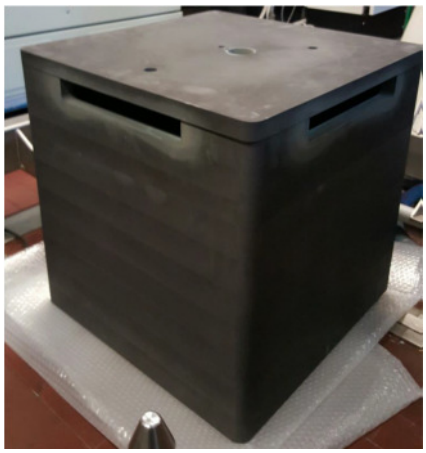

(c)

Figure 19: (a) Vacuum chamber,
(b) Upper and lateral inductor
(c) Susceptor box

G1 experiment

The utilization of a smaller G1crucible allows for installing a new side inductor for separation in the hot zone. This modification enables to apply higher frequencies up to 6 kHz where the Leenov-Kolin force will become large enough to promote particle separation. This experiment is supposed to allow for studying the superposition of Leenov-Kolin-force with tailored electromagnetic stirring. Figure 20 provides a drawing of the main components of the hot zone of Demonstrator II and their arrangement. The bottom support is needed because the G1 crucible has less height than the initially planned G2.5 size. Using the graphite susceptor plate at the top from the previously available system turned out to be the favoured solution for the initial melting of the silicon chunks. The carrier for it is a new part, in the previous installation the top susceptor rested on the graphite backup crucible. A serious problem is the substitution of the lateral graphite susceptors by alternative materials. Graphite cannot be used in the G1 experiment because of the shielding effect of high-frequency magnetic fields. Most difficult to produce and imposed to the highest stress is the vertical support frame. Since it is the only mechanically rigid structure between the quartz crucible softening in the elevated temperature range while containing the molten silicon and the copper coil carrying water, it determines the safety of the overall system in the majority. Therefore, new refractory materials have to be found being suitable to fulfill the mechanical requirements to sustain all the weight of the silica crucible filled with silicon.

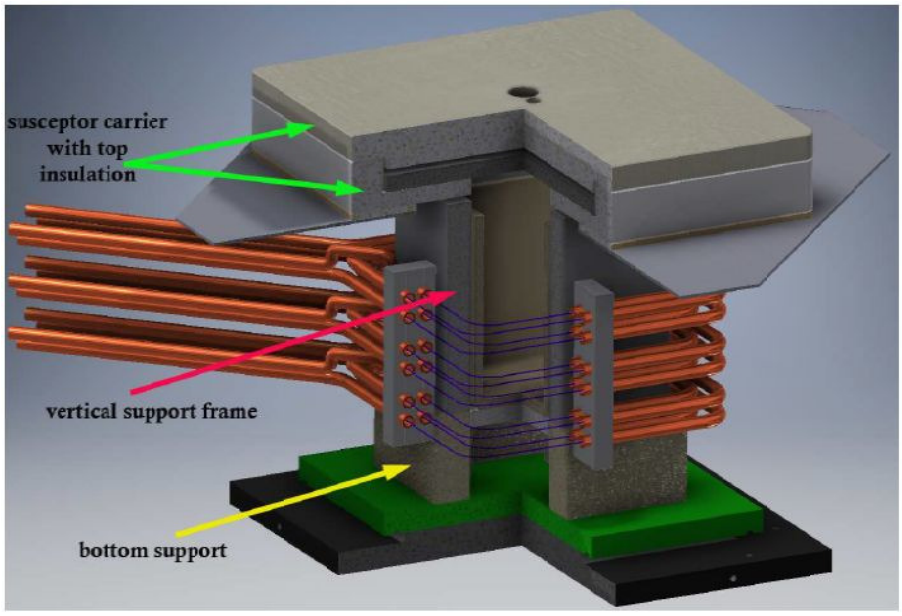

Figure 20: CAD drawing of the configuration of the G1 experiment (arrows point at the refractories under consideration)

The new ceramic material was tested by HZDR for manufacturing the refractory components of the hot zone. However, this ceramic contains Ca, Al and Fe oxides and therefore does not appear to be applicable for the hot zone. The use of such material bears the risk of contamination of the silicon. On the other hand, for safety reasons the G1 hot zone needs a component around the crucible which guarantees the mechanical stability of the crucible. Within SIKLEOR it was not possible to identify another candidate that meets all requirements. Thus, we had to conclude that there is no alternative solution with respect to a better suited material available within the duration of SIKELOR and the decision was made to go ahead with this ceramic.

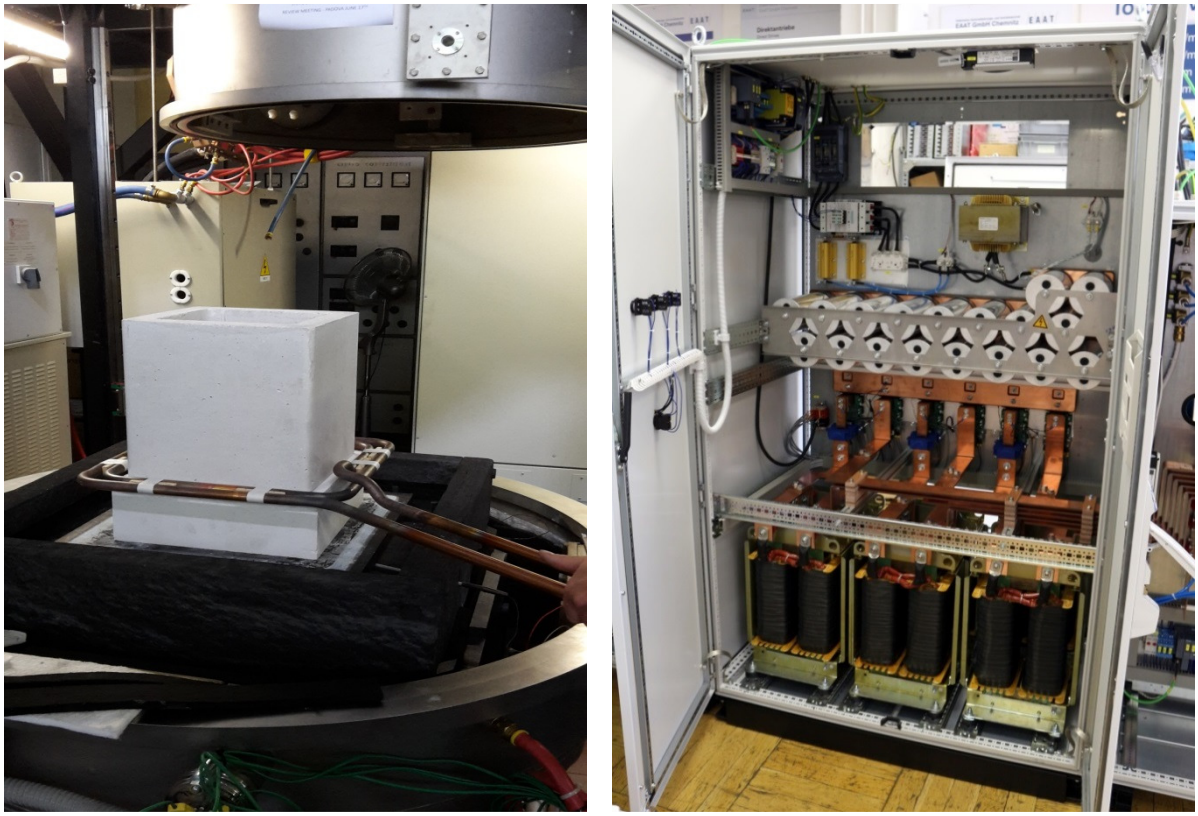

Figure 21: Assembling of the hot zone at the *i*DSS furnace at UNIPD (left), power cabinet of the EAAT power supply

Figure 21 illustrates the assembling of the hot zone for the G1 experiment. The experimental hardware is completed by a new power supply which is also shown in Figure 21. The demonstration of the electromagnetic separation of SiC particles in liquid silicon requires for designing and manufacturing a new type of electrical power supply by EAAT. The approach to superpose two or three magnetic fields presents challenges for the coil systems and the power supply comprising an entity of features not available commercially. The legal and economic starting conditions were determined by potentially available electrical sub-assemblies. The output of other work packages contributed to a specification of the features of the power supply. In particular, the results obtained by numerical modeling in WP 6 suggested that successful separation occurs at a relatively high frequency being in the same range as required for the inductive heating. Therefore, it was decided to design the power supply for generating a magnetic field containing two independent superimposed frequencies, a medium frequency for heating and separation (in the order of a few kHz) and a lower frequency for electromagnetic stirring. The power supply was designed to achieve a maximum frequency of 6 kHz, whereas a suitable frequency for stirring has to be distinctly below 200 Hz because of the shielding effect. An arbitrary tuning of both frequencies is possible.

Crystallization experiments

Crystallization experiments were performed inside the *i*DSS furnace at UNIPD using the G2.5 geometry. In our experiments the quartz crucible was filled by a 50:50 mixture composed of recycled silicon in form of a powder (supplied by GARBO) and new polycrystalline material in form of chunks (supplied by Wacker Chemie), respectively. The filling of the crucible with the 60 kg silicon is shown in Figure 22.

Figure 22: Charging of the crucible with 50% recycled material from GARBO on the bottom (left) and 50% new polycrystalline silicon from Wacker Chemie on the top (right)

The following process recipe was set in order to reproduce all steps of the directional solidification process:

- Heating at a controlled rate (150 K/hour) to avoid thermal stress widely on the silica crucible for about 10 hours
- Melting for about 4 hours
- Overheating of the top susceptor up to 1600°C
- Directional solidification for about 20 hours. The prelimi9nary tests were carried out with an average growth rate of about 0.8 mm/hour
- Annealing at 1050°C for about 4 hours
- Free cooling

This recipe is illustrated by the temperature measurements presented in Figure 23 showing the evolution of the local temperatures at the bottom and the top graphite susceptors. These temperature profiles at the top and bottom susceptors are specific for this experimental furnace and were successfully predicted by numerical simulations carried out at UNIPD. The flow rate of Argon gas was changed during the solidification according to the requirements.

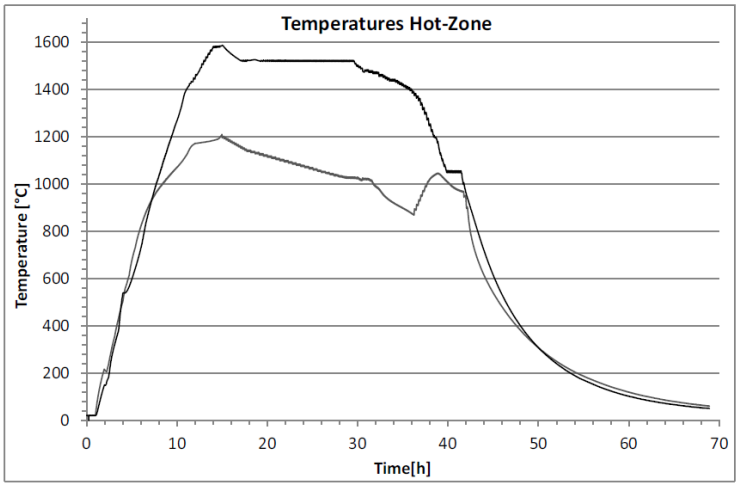

Figure 23: The process recipe: measured temperatures at the top and the bottom graphite suceptors

Between April and May 2016 three tests have been carried out in the G2.5 system. Even if the G2.5 was designed for melting and solidifying 120 kg of silicon feedstock, for safety reasons we limited the amount to 60 kg. The typical duration of one experiment was about 60 hours.
The first 60kg ingot cast in the *i*DSS furnace can be seen in Figure 24. This first test was very useful to improve the casting recipe (temperature vs time) mostly during the crystallization step. The other steps, the heating and melting as well as the final annealing were correctly performed.

Figure 24: First 60 kg ingot cast at the *i*DSS furnace at UNIPD

Figure 25 (left) shows the cross section and the side view of a brick having an area of $10 \times \text{cm}^2$ and a height of 5 cm. It becomes obvious that the crystal orientation is prevalently along the vertical line as desired. It is worth to note that a considerable amount of SiC is distributed on the top surface of the ingot. On the top of the silicon ingot and in the cold part of the vacuum chamber there was also a significant quantity of silicon nitride found. A respective photograph of the ingot surface is also presented in Figure 25 (right).

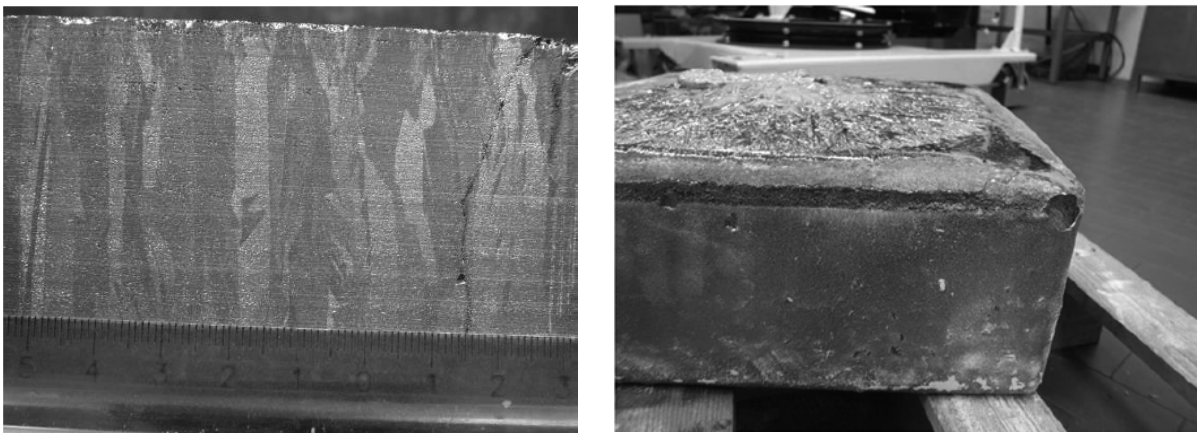

Figure 25: Side view of the brick truncated from the ingot (left), photograph showing the ingot casted in Demonstrator II

Exemplary results from metallographic and chemical analysis of the powders deposited on the ingot top surface are presented in the Figures 26 and 27. The spectrum of the green powder shown in Figure 26 reveals distinct peaks for silicon and carbon which implies a definite identification of SiC. Figure 27 (left) contains a SEM image (Cambridge Stereoscan 440 SEM and probe EDS Philips PV9800) of the black powder from the top of the ingot. The peaks for silicon and nitrogen in the corresponding spectrum (see Figure 27, right) suggest the

occurrence silicon nitride. The silica crucible is coated with a thick layer of silicon nitride acting as anti-adhesion layer. The fact that silicon nitride is found as black powder on the ingot and the problem of the local sticking of the silicon at the crucible walls indicates problems with respect to a non-perfect coating process or a detachment of the coating from the silica which might be induced by a strong motion induced in the liquid bath.

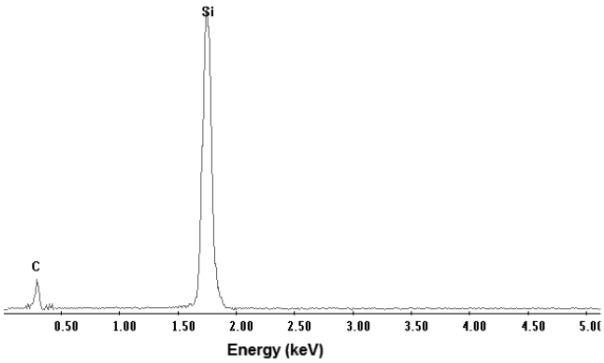

Figure 26: Spectrum of the green powder (SiC) on the top of the ingot

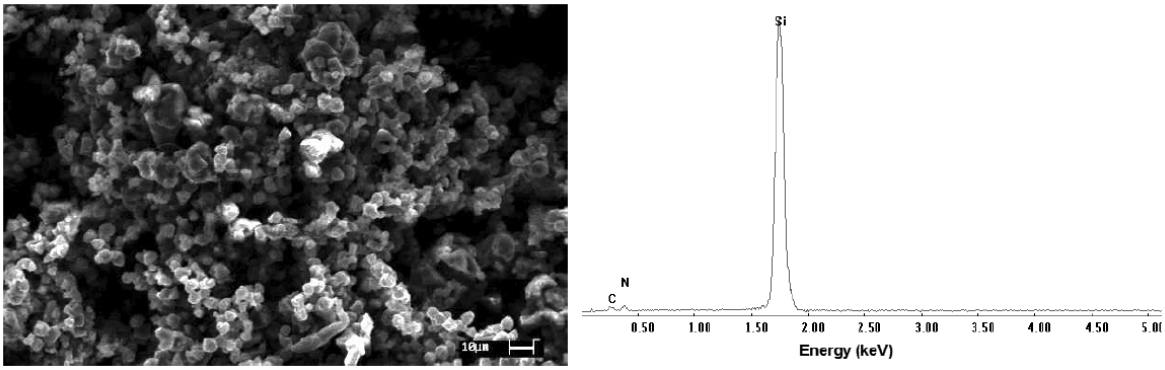

Figure 27: SEM image of black powder (silicon nitride) on the top of the ingot (left) and the corresponding spectrum (right)

The ingots were cut into four bricks (see Figure 28) and analyzed by Fraunhofer Center for Silicon Photovoltaics in Halle (Germany). The results show that a significant amount of silicon carbide pollutes the silicon crystals. This outcome demonstrates the necessity of improving the quality of the material by separating SiC particles from the Si during the solidification. Infrared measurements without grinding were not successful. Therefore, a pre- and fine-grinding procedure was applied for all four sides.

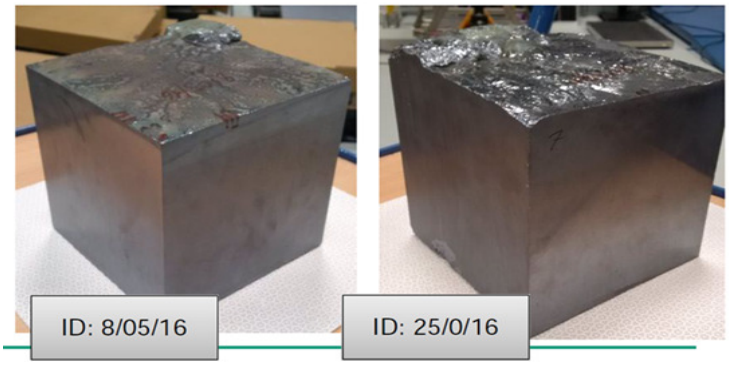

Figure 28: Silicon bricks prepared for infrared analyis

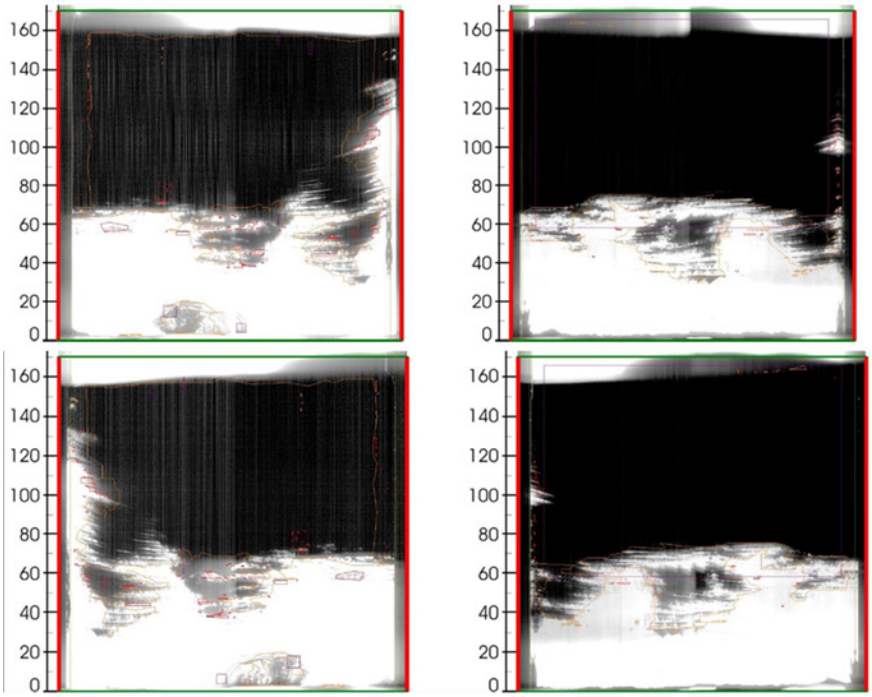

Figure 29: Shadowgraphs showing the results of the infrared measurements: virgin feedstock

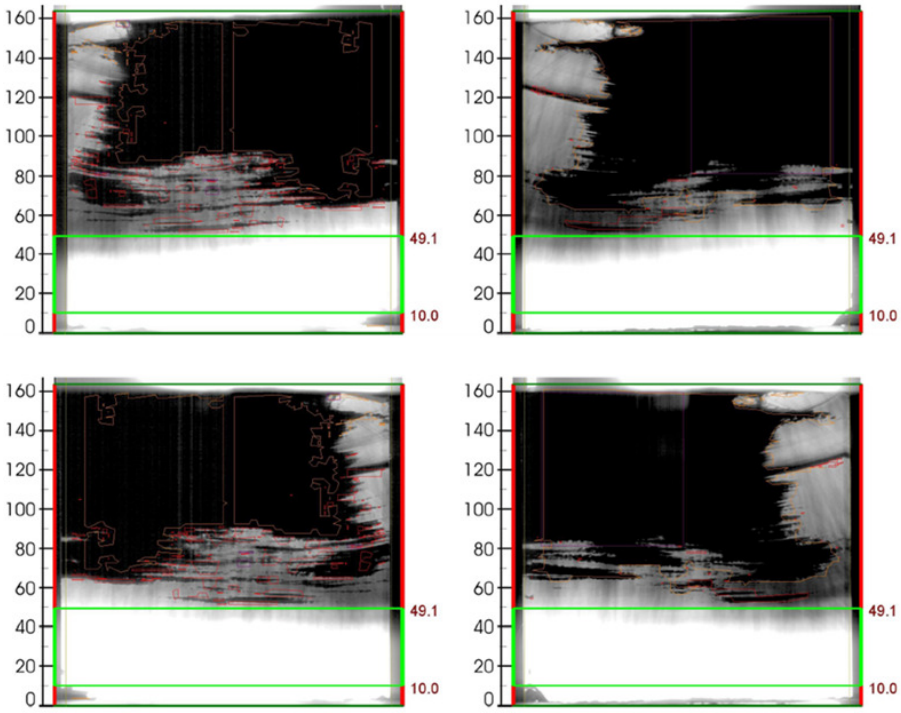

Figure 30: Shadowgraphs showing the results of the infrared measurements: 50:50 mixture composed of recycled silicon and new polycrystalline material

The infrared analysis performed by CSP Halle demonstrated the high amount of SiC present in both the tests, but, surprisingly, the ingot casted with recycled material showed a little bit lower content of SiC mostly in the bottom part of the ingot. The corresponding results are compared in the Figures 29 and 30, respectively

Objectives, which were not or only partially achieved

Not all objectives were achieved as planned at the beginning of the project. A description of failures and unexpected developments has been given in the Second Periodic Report. Here, we will summarize the status of the related main objectives.

a) Crystallization experiments in Demonstrator II

The crystallization experiments could not be completed during the course of the SIKELOR project. The original plan considered to deploy the available setup of the *i*DSS furnace at UNIPD. However, new insights obtained during the first stage of the project required significant changes of the inductor and the hot zone. A drastic consequence was the decision made within the consortium to perform experiments in the existing G2.5 geometry and to prepare in parallel a new G1 setup. This decision was driven by the newly gained insight that a separation of the solid particles cannot be achieved by the existing construction of the hot zone and the inductor. The technical details are described in the Second Review Report.

First crystallization experiments were successfully carried out in the G2.5 geometry. The results for three solidified ingots are presented in the Second Review Report. As mentioned above, for these experiments it was not possible to generate magnetic field conditions being promising for an efficient separation of SiC particles. The ingots were analysed by the Fraunhofer Center for Silicon Photovoltaics in Halle (Germany). Consequently, the results showed a non-negligible contamination of the ingots by SiC and silicon nitride (SiN). This outcome demonstrates the necessity of improving the quality of the material by separating SiC particles from the Si during the solidification. The occurrence of SiN can be attributed to the coating of the silica crucible with a thick layer of silicon nitride acting as anti-adhesion layer. The detection of the black SiN powder on the ingot and in the cold part of the vacuum chamber indicates problems with respect to the crucible coating. This concern is strengthened by the observation of a local sticking of the silicon at the crucible walls. At the moment it is not clear whether the problem is caused either by 1) a non-perfect coating process, or 2) the detachment of the coating from the silica could be induced by a strong motion induced in the liquid bath. Further tests will be necessary to clarify this aspect. Moreover, the risk of damaging the crucible coating by a non-controlled fluid flow near the crucible wall has to be taken into consideration for the concept of electromagnetic stirring of the silicon.

The G1 variant of Demonstrator II enables us for realizing a combination of TMF and AMF which is supposed to provide both a sufficiently strong LKF for particle separation and an intense electromagnetic stirring. The new hot-zone of the G1 experiment overcomes the problem of the G2.5 setup with respect to the shielding of high-frequency magnetic fields by the graphite components. Moreover, UNIPD performed an additional risk analysis taking into account undesired events such as crucible failure, breakage of susceptors, internal water leaks, high pressure inside the chamber and power failure. Moreover, the G1 experiment in the Demonstrator II is capable to conduct all experiments foreseen for Demonstrator I. In a majority of details, e.g., the field strength, the control over the fluid velocity, and problems with the pole pitch of the TMF coils in the Demonstrator II is even superior to the features considered in Demonstrator I. The unforeseen effort and costs for designing and constructing the new setup for G1, the late delivery of the new power supply as well as the sophisticated safety analysis caused a remarkable delay in the schedule of the experimental work program. At the end of the project the new setup has been completed and tested. The new power supply delivered by EAAT has also been installed and tested. However, it was not possible to schedule the first crystallization experiments in the G1 setup during the official project period of SIKELOR. The G1 experiment was not planned in the original work program and required additional time and resources. For example, the hot-zone had to be completely redesigned. Additional problems were caused by the need to replace the graphite susceptor with

alternative materials. In addition, the complete modification of the experiment caused a reassessment of the requirements to the power source and the safety questions of the test facility. This all together generated a significant time delay in the work program. Therefore, at that stage the SIKELOR project gave no definite answer to what extent the LKF is capable to contribute to the purification of silicon in relevant sizes of the melt volume.

Moreover, the material issue due to the substitution of graphite in the hot zone has to be considered as a serious problem and one of the main disadvantages within the project. During the course of the project it became obvious that there is no alternative material available on the market which could meet the following requirements:

- To allow high-frequency magnetic fields to pass through,
- To guarantee the stability and safety of the hot zone, and
- To guarantee the purity of the melt and to be accepted by the silicon industry.

As a viable alternative, SIKELOR deployed a ceramic material which fulfils the first two demands, but, implicates contamination hazards by elements such as Ca, Al and Fe. It was not possible to solve this problem within SIKELOR, because the consortium does not comprise a relevant competence in the field of new material development. This issue has to be taken into account by future research projects dealing with applying high-frequency magnetic fields for reasons of process control in silicon melts.

b) Demonstrator I

Design and modeling work and estimates done within the project revealed that an efficient and successful operation of the magnetic system in Demonstrator I with respect to particle separation can only be guaranteed by means of an internal metallic coil system. However, this option was refused by GARBO because of the risk of contamination. The impact and scientific outcome of crystallization experiments under the effect of weak magnetic fields generated by graphite coils in GARBO's furnace would have been limited. Analyzing this situation the project partners came to the conclusion to abandon Demonstrator I in the form as initially planned. The project objectives were transferred to the experiments performed in Demonstrator II. The G1 experiment in Demonstrator II offers an application of both TMF and AMF in a wide parameter range which is even superior to the one considered in Demonstrator I. All the investigations to be expected in Demonstrator I regarding TMF-driven fluid flow can be even better achieved with the hardware of Demonstrator II. As a compensation for the research activities associated with the cancelled Demonstrator I, GARBO performed additional sintering experiments aimed to reduce the content of oxygen in the compacted kerf loss before the electromagnetic processing and casting stages.

c) Model experiments

Model experiments were planned for validation of the numerical simulations done in WP6 and for supporting the design of the magnetic field for Demonstrator I. For the verification of the numerical code flow measurements were performed successfully using a generic setup comprising a cylindrical vessel situated within an arrangement of Helmholtz coils. For the first time, systematic measurements were carried out by means of the ultrasound Doppler method revealing the spatio-temporal flow structure for the specific case of an alternating magnetic field (AMF) at high frequencies implying high shielding parameters, in contrast to previous studies where only an incomplete pointwise representation of the flow pattern was detected at selected positions. Consequently, our measurements revealed the existence of a more complicated flow field topology at high shielding parameters which differ significantly from the previously known time-averaged flow structures as given in the literature so far. We observed rather complex, transient vortex structures from which a significant mixing effect by the AMF can be deduced.

In WP7 a more realistic experimental configuration was considered with respect to the design of both the Demonstrators and industrial facilities. In particular, the equipment comprises a quadratic side coil, a quadratic fluid vessel (size G1) and a more efficient power supply. However, because of the cancelation of Demonstrator I the related model experiments were suspended. Corresponding man power was transferred to WP8 to support the construction of Demonstrator II. In view of the encouraging new results obtained by the first tests, HZDR decided to continue the program of the model experiments beyond the end of the SIKELOR project. The first measuring campaign was completed at the end of January 2017. The results of the measurements will be shared with the project partners.

Further prospects for success

The knowledge and numerical predictions gained during SIKELOR give rise to optimistic expectations that the capability of LKF for the separation of SiC particles in silicon melts can be demonstrated by the G1 experiments in Demonstrator II. The research partners (UNIPD, UNIG and HZDR) decided to continue the work on this topic on their own responsibility after the end of SIKELOR. Particularly, UNIPD plans to carry out series of crystallization experiments in Demonstrator II. The analysis of the solidified ingots should provide useful data concerning the material purity achieved for different processing conditions. This work will be done in close contact to UNIG. It should be checked whether the recipes proposed for the electromagnetic processing of the ingots can be approved. UNIG will support the experiments with further simulations for an adaptation and optimization of the recipes and an interpretation of the results.

The industrial partners (GARBO and EAAT) will be kept informed about the progress of further work and the upcoming results. At the appropriate time a decision will be made how to proceed. Provided that successful crystallization experiments can be done in the Demonstrator II the partners will consider the option to apply for another follow-on project.

Explanation to budgetary changes, redistribution within SIKELOR

SIKELOR was planned as a research project which had to master a balancing act to design and realize demonstrators for the purification of liquid silicon on one hand, while to investigate fundamental aspects of the electromagnetic processing of particle-laden fluids on the other hand. Therefore, a couple of questions were raised at the very beginning of the project. The most prominent findings which lead to unforeseen consequences in the work program were:

- the new flow structures found in the numerical simulations and the model experiments, which are a novelty for the silicon casting applications
- the fact that effective separation can only be obtained at significantly higher frequencies as those suggested by previous studies in the available literature and, henceforth, expected at the time of the application writing, and
- the numerical and technical insights that the graphite coils initially proposed for the Demonstrator I at GARBO cannot provide sufficient electromagnetic agitation of the melt. The related upgrade of the GARBO furnace by metallic coils could not be realized within the technical and budgetary bounds of the project.

A possible weakness of the initial SIKELOR application could have been traced a posteriori to the impact of unforeseen changes and the related risks not balanced by adequate reserves in both the schedule and the budget.

For instance, the above mentioned findings caused changes with respect to the requirements for the power source design. These changes and the repeated rescheduling of the parameter

choice created an extra effort and expenses for the partner EAAT. In particular, 157.300 € were planned for the man power, 190.010 € were spent actually. 36.000 € were planned for consumables, 83.139 € were spent actually. A better planning of the costs was hardly possible because the specification of the features and parameters was not available when applying for the project. A partial absorption of the additional costs by HZDR is planned in the course of the final payment arrangement.

The findings of SIKELOR that the operating range for the particle separation has to be shifted to higher frequencies required a new power supply for the model experiments at HZDR, too. The costs for this new power supply delivered by EAAT (~ 60.000 €) were covered by HZDR and have not been claimed within the SIKELOR project.

The cancelation of Demonstrator I in WP 7 released resources at HZDR and GARBO. These resources were redirected within SIKELOR in order to ensure the achievement of the main project objectives.

I) GARBO performed additional sintering experiments
The additional sintering procedure improves the density of the compacts allowing a higher crucible filling factor and reduces a certain amount of oxygen ahead of the electromagnetic processing and casting.

II) The realization of the Demonstrator II at Padova was supported by GARBO and HZDR
The requirement for adjusting higher frequencies for particle separation provoked a complete new construction of the hot zone. The graphite susceptor had to be substituted by an alternative material which is stable and does not shield the magnetic field. Manpower costs from the HZDR planned for Demonstrator I were used to contribute in designing and building the new hot zone for Demonstrator II, in particular the ceramic components of the hot zone and the steel frame were made at HZDR. The corresponding costs for consumables (~ 4.500 €) were also covered by HZDR. GARBO supported the construction of Demonstrator II by man power and paid for the crucibles (~5.900 €).

III) In the course of the final payment it is planned to transfer money to EAAT to cover the incremental costs of the power supply (see above).

UNIPD had to cover additional costs to realize the set-up of the G1 experiment in Demonstrator II. Although the possibility for only minor modifications of the inductor was foreseen in the work plan, a very complex coil had to be realized in order to achieve sufficiently high magnetic field intensities. Further modifications of the cooling system, the cable system and connections were necessary. The additional total direct costs add up to about 20 k€, including additional man power.

The procedure of the redistribution of the budget was discussed among the partners and decided during the project meetings.

References

[6] S. Meyer, S. Wahl, A. Molchanov, K. Neckermann, C. Möller, K. Lauer, C. Hagendorf: „Influence of the feedstock purity on the solar cell efficiency.“ *Solar Energy Materials and Solar Cells* **130** (2014) 668-672.

[7] A.K. Søiland, J. O. Odden, B. Sandberg, K. Friestad, J. Håkedal, E. Enebakk, S. Braathen: "Solar silicon from a metallurgical route by Elkem solar – a viable alternative to virgin polysilicon." In *6th International Workshop on Crystalline Silicon Solar Cells, CSSC 6, Aix les Bains* (2012).

[8] D. Leenov, A. Kolin: “Theory of electromagnetophoresis. Magnetohydrodynamic forces experienced by spherical and symmetrically oriented cylindrical particles.” *J. Chem. Phys.* 22 (1954) 683–688.

[9] P. Marty, A. Alemany: “Metallurgical Applications of Magnetohydrodynamics:” *Proc. of the IUTAM Symposium, The Metals Society London* (1984) 245-259.

[10] A. Cramer, C. Zhang, S. Eckert: „Local flow structures in liquid metals measured by ultrasonic Doppler velocimetry.“ Flow Meas. Instrum. **15** (2004) 145-153.

[11] M. Kadkhodabeigi, J. Safarian, H. Tveit, M. Tangstad, S.T. Johansen: “Removal of SiC particles from solar grade silicon melts by imposition of high frequency magnetic field.” *Trans. Nonferrous Met. Soc. China* **22** (2012) 2813–2821.

[12] S. Wang, L. Zhang, Y. Tian, Y. Li, H. Ling: “Separation of non-metallic inclusions from steel using high frequency electromagnetic fields.” *Metall. Mater. Trans. B* **45** (2014) 1915–1935.

[13] E.D. Tarapore, J.W. Evans: “Fluid velocities in induction melting furnaces: Part I. Theory and laboratory experiments.” *Metall. Trans. B* **7** (1976) 343–351.

[14] E. Taberlet, Y. Fautrelle: “Turbulent stirring in an experimental induction furnace.” *J. Fluid Mech.* **159** (1985) 409–431.

[15] S. Taniguchi, N. Yoshikawa, K. Takahashi: “Application of EPM to the separation of inclusion particles from liquid metals.” *Proc. of the 6th Int. PAMIR conf. on fundamental and applied MHD, Riga* (2005), 55-63.